

Chapter 10

DISORDER

Order is associated with symmetry, beauty and simplicity. Some of the most profound advances in physics have exploited these concepts to help understand fundamental issues about space and time, as well as the structure of matter at the elemental scale. On the other hand, the notion of disorder resonates with chaos, confusion, and complexity. Such prejudices hindered scientific progress about disordered systems, and systematic efforts to solve specific models of disordered media—apart from a few pioneering papers in earlier decades—began in the mid 1970's. Quite surprisingly, it was found that many disordered systems exhibit astonishingly beautiful behaviors that rival the properties of the most symmetrical and ordered systems. It was also realized that in disordered systems, dynamical properties are usually much more important than in ordered systems. For many disordered systems, the dynamical behavior is absolutely crucial; for example, glasses apparently *cannot* be treated adequately within an equilibrium framework.

One prejudice about disordered systems, namely the concern that they can be extraordinarily complicated, perhaps does reflect reality. There is still much effort in constructing “good” models—namely, models that capture the physical essence of how disorder affects a physical phenomenon but that are simple enough to be solved analytically or simulated to a reasonable time scale. As a consequence, many physical properties of disordered systems are still poorly understood. Even for spin glasses—a very special and simple type of glass system—little concrete knowledge has been gained despite three decades of research.

A particularly simple example of a disordered spin system is the Ising model with non-uniform interactions. This system is described by the Hamiltonian

$$\mathcal{H} = - \sum_{\langle ij \rangle} J_{ij} s_i s_j \quad (10.1)$$

in which the interactions J_{ij} between neighboring spins s_i and s_j are *random*, rather than taking a single value. We shall always assume J_{ij} to be independent identically distributed random variables. A weakly disordered system in which the interactions all have the same sign is known as a random ferromagnet. Here we might still expect ferromagnetic order at low temperature, and a basic question is how does the disorder affect the transition. When the interactions are both ferromagnetic ($J_{ij} > 0$) and antiferromagnetic ($J_{ij} < 0$) with sufficiently similar overall strengths, the low-temperature phase is much more complex. There is no long-range ferromagnetic order, but rather, *spin-glass* order arises in which each spin tends to align with its local (but randomly oriented) field. The properties of the phase transition and the spin glass phase are difficult to access experimentally, numerically, and theoretically, a fact that has helped perpetuate the mystery of spin glasses. Three-dimensional spin glasses undergo this transition to a spin glass phase at a positive temperature. The situation is much simpler in lower dimensions where the phase transition occurs at zero temperature.

In this chapter we give some glimpses into the rich world of disordered systems by studying the simplest possible systems where disorder plays an essential role in the dynamical behavior.

10.1 Disordered Spin Chains

In one dimension, many aspects of the disordered Ising model are tractable analytically. Here we focus on the long-time evolution of the system when individual spins evolve by Glauber dynamics. We impose no conditions on the distribution $\rho(J_{ij})$ of interactions apart from the requirement that $\rho(J_{ij})$ does not contain any delta function component. This constraint ensures that the interactions between different pairs of spins are never equal. Thus every spin flip either raises or lowers the energy, while the probability of an energy conserving move is zero. Sometimes, we shall assume that the distribution is symmetric $\rho(J_{ij}) = \rho(-J_{ij})$ but most of our results apply to arbitrarily disordered spin chains.

As in the case of a translationally invariant system, the phase transition to an ordered state occurs at zero temperature in one dimension. The interesting dynamical behavior also occurs at zero temperature, and we therefore set $T = 0$ henceforth. There are two basic questions that we can answer about the one-dimensional disordered Ising model. The first is the structure of state space. In contrast to the homogeneous Ising model, there are many metastable states in the disordered Ising model. The second and surprising feature is the long-time magnetization of the system; in fact, the final magnetization is *independent* of all system details!

Metastable States

Let's first determine on the ultimate fate of a disordered Ising chain. At zero temperature, energy raising spin flips are forbidden. so that the system eventually reaches a *metastable* state where energy lowering single-spin flips are no longer possible. For the ferromagnetic Ising chain, there are exactly two metastable states—the ground states. For the disordered spin chain, there are many more metastable states that we can enumerate by the following approach. In a metastable state, each spin is aligned with its local field. That is, the state of the i^{th} spin is determined by

$$s_i = \text{sgn}(J_{i-1}s_{i-1} + J_i s_{i+1}), \quad (10.2)$$

where $J_i \equiv J_{i,i+1}$. Since $|J_{i-1}| \neq |J_i|$ with probability 1, only the stronger of the two bonds matters; for example, if $|J_i| > |J_{i-1}|$, then (10.2) gives $s_i = \text{sgn}(J_i s_{i+1})$, *i.e.*, s_i is perfectly coupled to s_{i+1} .

To characterize the metastable states, it is useful to compare the strength of each bond with those of its two adjacent bonds. We term the i^{th} bond as “strong” if $|J_i| > \max(|J_{i-1}|, |J_{i+1}|)$. Similarly the bond is called “weak” if $|J_i| < \min(|J_{i-1}|, |J_{i+1}|)$. Otherwise, the bond is “medium”. In determining the final state of the system, the actual bond strength is irrelevant; the only feature that matters is whether it is weak, medium, or strong. Therefore the bond configuration can be equivalently represented as a word in an alphabet consisting of the three letters, W, M, S (Fig. 10.1).

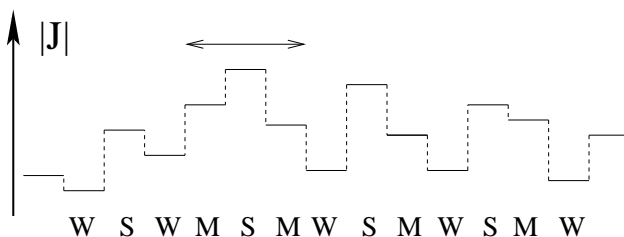


Figure 10.1: The landscape of the bond strengths $|J_i|$ showing the representation in terms of a three-letter alphabet— W, M, S —for weak, medium, and strong bonds. A cluster of 3 bonds and 4 sites is shown (double arrow).

We define the part of the chain between two consecutive but non-adjacent weak bonds as a *cluster*. There is exactly one strong bond in a cluster. Likewise, there is exactly one weak bond between two consecutive, non-adjacent strong bonds. Consider the i^{th} bond and suppose it is not weak. Hence it is stronger than at least one adjacent bond, say $|J_i| > |J_{i-1}|$. Then $s_i = \text{sgn}(J_i s_{i+1})$, that is, for a ferromagnetic bond ($J_i > 0$) the spins are parallel ($s_i = s_{i+1}$), while for an antiferromagnetic bond the spins are antiparallel. The i^{th} bond is therefore *satisfied*. If the bond is weak, the end spins are unrelated and the bond could equally

well be satisfied or *frustrated*. Since the state of each weak bond may be specified independently, the total number of metastable states is

$$\mathcal{M} = 2^\Omega, \quad \Omega = \text{number of weak bonds.} \quad (10.3)$$

Now we need to relate Ω to the number of spins in the system. This can be done by the following combinatoric argument. Consider three consecutive bonds. What is the probability that a weak bond exists in this group? By definition, a weak bond would have to be both in the center of the group and the weakest among the three bonds. There are $3!$ permutations of the bond alphabet for this cluster: WMS , WSM , MSW , MWS , SWM , and SMW . Of these, only in the configurations MWS and SWM are we assured that the bond with the smallest interaction strength is truly a “weak” bond. Thus the probability of finding a weak bond in any 3-bond cluster is $1/3$ and the average number of weak bonds is $N/3$. Therefore the typical number of metastable states grows with the system size N as

$$\mathcal{M}_{\text{typ}} \propto 2^{N/3}. \quad (10.4)$$

Evolution

An important and experimentally relevant question for the evolution of a spin glass is the *remanent magnetization*. This quantity is defined by preparing a laboratory spin glass in well magnetized state, typically by applying a very large external magnetic field. Then the field is switched off, keeping the temperature fixed, and one waits until the system relaxes to its final state. The residual magnetization at infinite time is the remanent magnetization, $m_\infty = m(t = \infty)$. Generally, the remanent magnetization also depends on the temperature at which the experiment is performed.

By the nature of the experimental conditions, the remanent magnetization probes the structure of the phase space and provides information about the typical metastable states of the system. The nature of metastable states are extraordinarily complex for a real spin glass, but as discussed in the previous section, the situation simplifies greatly in one dimension. As we now discuss, the remanent magnetization has a remarkably simple behavior in a one-dimensional spin glass.

As discussed above, the Ising chain spin glass effectively breaks up into non-interacting clusters that are delimited by two consecutive weak bonds. Each cluster contains one strong bond and some (perhaps none) medium bonds; thus a cluster contains at least 2 spins. Let us now determine the evolution of each cluster according to single spin-flip zero temperature dynamics.

Consider a cluster that contains ℓ spins s_1, \dots, s_ℓ . Suppose that the bond across $(j, j + 1)$ is strong. Then in an infinitesimal time interval dt a spin s_i with $1 \leq i \leq j$ (to the left of the strong bond) changes as follows:

$$s_i(t + dt) = \begin{cases} s_i(t) & \text{probability } 1 - dt \\ \epsilon_i s_{i+1}(t) & \text{probability } dt, \end{cases} \quad (10.5)$$

where $\epsilon_i \equiv \text{sgn}(J_i)$. The second line in Eq. (10.5) accounts for the fact that in an update event s_i equals s_{i+1} , if there is a ferromagnetic interaction between the two spins, while $s_i = -s_{i+1}$, if there is an antiferromagnetic interaction. Thus we find that $S_i(t) \equiv \langle s_i(t) \rangle$ satisfies

$$\frac{dS_i}{dt} = -S_i + \epsilon_i S_{i+1}, \quad 1 \leq i \leq j. \quad (10.6)$$

Similarly, spins with $j + 1 \leq i \leq \ell$ (to the right of the strong bond) change according to

$$\frac{dS_i}{dt} = -S_i + \epsilon_{i-1} S_{i-1}, \quad j + 1 \leq i \leq \ell. \quad (10.7)$$

What we want to understand is the evolution of the macroscopic system. This means that we should perform the average over the distribution of interactions. Since the interactions are independent identically distributed (iid) random variables, the ϵ_i are also iid that take the values ± 1 only. We now additionally assume that the distribution of interactions, $\rho(J_i)$, is symmetric; then the ϵ_i equal ± 1 independently and with equal probability.

Let $\overline{(\dots)}$ denote averaging a quantity (\dots) over the distribution of interactions. Thus $\bar{\epsilon} = 0$ by definition. Instead of solving Eqs. (10.6)–(10.7) and then averaging the solutions over the disorder, we first average these equations and then solve. The averaging of linear terms simply gives $S_i \rightarrow \overline{S}_i$, and averaging the quadratic terms is also simple since the factors in products are uncorrelated. For example, $\overline{\epsilon_i S_{i+1}} = \bar{\epsilon}_i \overline{S}_{i+1} = 0$ for $i < j$. Thus S_{i+1} depends on ϵ_{i+1} and S_{i+2} , but in turn, S_{i+2} in turn depends on ϵ_{i+2} and S_{i+3} , etc. Therefore S_{i+1} depends on $\epsilon_{i'}$ with indices $i' \geq i+1$. Because different ϵ 's are independent, we conclude that ϵ_i and S_{i+1} are uncorrelated. Averaging (10.6)–(10.7) we obtain simply

$$\frac{d}{dt} \overline{S}_i = -\overline{S}_i \quad \text{for all } i \neq j, j+1,$$

with solution $\overline{S}_i(t) = \overline{S}_i(0) e^{-t}$.

For the two spins attached to the strong bond $(j, j+1)$, the above procedure does not quite work because s_{j+1} is now determined by its left neighbor s_j . We can, however, directly solve the original equations

$$\frac{dS_j}{dt} = -S_j + \epsilon_j S_{j+1}, \quad \frac{dS_{j+1}}{dt} = -S_{j+1} + \epsilon_j S_j \quad (10.8)$$

and then perform the averaging. Suppose that the initial state is aligned: $s_i(0) = 1$ for all i . Then by adding and subtracting the two equations in (10.8) we ultimately obtain $S_j = S_{j+1} = e^{(\epsilon_j - 1)t}$. Averaging over the disorder, the average spin values within a cluster are therefore

$$\overline{S}_j = \overline{S}_{j+1} = \frac{1 + e^{-2t}}{2}, \quad \overline{S}_i = e^{-t} \quad \text{for } i \neq j, j+1$$

In a cluster of ℓ spins, the two spins at the ends of the strong bond evolve according to the first formula and the remaining $\ell - 2$ spins follow the exponential relaxation. Let NX_ℓ be the number of clusters that contain ℓ spins. The average magnetization is then given by summing over all possible cluster sizes

$$m(t) = (1 + e^{-2t}) \sum_{\ell=2}^{\infty} X_\ell + e^{-t} \sum_{\ell=2}^{\infty} (\ell - 2) X_\ell. \quad (10.9)$$

The first sum in (10.9) is the density of clusters. Because of the one-to-one relation between clusters and weak bonds, the cluster density also equals the density of the weak bonds; hence $\sum_{\ell \geq 2} X_\ell = \frac{1}{3}$. Using this result, together with the normalization $\sum_{\ell \geq 2} \ell X_\ell = 1$ we find that the second sum in (10.9) is $\sum_{\ell \geq 2} (\ell - 2) X_\ell = \frac{1}{3}$. Thus the magnetization is simply

$$m(t) = \frac{1 + e^{-t} + e^{-2t}}{3},$$

so that the remanent magnetization is

$$m_\infty = \frac{1}{3}$$

Both these results are remarkably universal, that is they are completely independent of the distribution of interaction strengths.

As a side note, the cluster size distribution itself is also independent of the distribution of interaction strengths and equals

$$X_\ell = 2^\ell \frac{(\ell - 1)(\epsilon; +2)}{(\ell + 3)!} \quad (10.10)$$

The form of this remarkable formula suggests that it ought to admit a conceptual derivation; the only currently known derivation involves detailed calculations.

Let now compute the final energy per spin \mathcal{E} . Each weak bond is satisfied or frustrated equiprobably, so the corresponding contribution to energy vanishes. All non-weak bonds are satisfied and the fraction of such bonds is $2/3$ leading to $\mathcal{E} = -\frac{2}{3} \overline{|J|_{nw}}$. Adding and subtracting $\frac{1}{3} \overline{|J|_w}$, and noting that $\frac{2}{3} \overline{|J|_{nw}} + \frac{1}{3} \overline{|J|_w} = \overline{|J|}$, gives

$$\mathcal{E} = -\overline{|J|} + \frac{1}{3} \overline{|J|_w} \quad (10.11)$$

The probability density function for the absolute value of the coupling strength is $\psi(x) = \text{Prob}(|J| = x)$, while for the weak bond $\text{Prob}(|J|_w = x) = \psi(x) \left\{ \int_x^\infty dy \psi(y) \right\}^2$. Therefore (10.11) becomes

$$\mathcal{E} = - \int_0^\infty dx x \psi(x) + \frac{1}{3} \int_0^\infty dx x \psi(x) \left\{ \int_x^\infty dy \psi(y) \right\}^2$$

The above computation applies for an arbitrary metastable state. Thus almost all metastable states have the same energy which is larger than the ground state energy $\mathcal{E}_{GS} = -\overline{|J|}$. For instance, for the uniform coupling distribution $\psi(x) = 1$ for $0 \leq x \leq 1$ and zero otherwise, the ground state energy is $\mathcal{E}_{GS} = -\frac{1}{2}$, while almost all metastable states have the energy $\mathcal{E} = -\frac{17}{36}$; for the exponential distribution $\psi(x) = e^{-x}$ we get $\mathcal{E}_{GS} = -1$ and $\mathcal{E} = -\frac{26}{27}$.

10.2 Heterogeneous Random Walks

Heterogeneous step lengths

A profound and remarkable fact about random walks is that the probability distribution of displacements after a large number of steps converges to a universal Gaussian distribution, independent of the form of the single step distribution (subject to a mild restriction to be discussed below). This fact is known as the *central limit theorem*. To simplify the discussion, suppose that the walk is confined to one dimension and takes steps at discrete times, with the displacement of each step x is chosen from a distribution $p(x)$. Let $X_N = \sum_{n=1}^N x_n$ be the displacement of a random walk after N steps. Then the precise statement of the central limit theorem is that the asymptotic $N \rightarrow \infty$ probability distribution of the total displacement, $P(X_N)$, is the *universal Gaussian* function

$$P(X_N) \sim \frac{1}{\sqrt{2\pi N\sigma^2}} e^{-(X_N - N\langle x \rangle)^2 / 2N\sigma^2} \quad \sigma^2 \equiv \langle x^2 \rangle - \langle x \rangle^2, \quad (10.12)$$

as long as the first two moments of the single-step distribution

$$\langle x \rangle = \int_{-\infty}^{\infty} x p(x) dx \quad \text{and} \quad \langle x^2 \rangle = \int_{-\infty}^{\infty} x^2 p(x) dx,$$

are finite. Eq. (10.12) tells us that the mean displacement after N steps is simply $\langle X_N \rangle = N\langle x \rangle$ and that the variance is $\text{var}(X_N) = N\sigma^2$.

What happens when the displacement distribution in a single step is sufficiently broad that the above two conditions on the first two moments are violated? As we now discuss, the distribution $P(X_N)$ is no longer Gaussian and the moments of the N -step displacement scale anomalously with N . These two features arise because a sufficiently broad distribution of single-step displacements can give rise to an exceptionally long step that comprises a finite fraction of the total displacement. The existence of such an exceptional event invalidates the conditions that lead to the central limit theorem.

To make our discussion concrete, suppose that the single-step distribution is given by $p(x) \propto x^{-(1+\mu)}$, with $\mu > 0$, for $x > 1$. We impose a lower cutoff $x > 1$ on the step length to avoid potential singularities associated with very short steps. Instead of attempting a direct calculation of the moments of the N -step displacement, we exploit a simple application of extreme value statistics to determine these moments in a physically appealing way. We first estimate the largest step length during a walk of N steps, $x_{\max}(N)$, by the extremal criterion:

$$\int_{x_{\max}}^{\infty} x^{-(1+\mu)} dx = \frac{1}{N}. \quad (10.13)$$

This statement mandates that one of the steps in an N -step walk has length greater than or equal to x_{\max} . From Eq. (10.13), we immediately find that $x_{\max} \sim N^{1/\mu}$. Thus for an N -step walk, the effective single step distribution is

$$p(x) = \begin{cases} \frac{\mu}{1 - x_{\max}^{-\mu}} x^{-(1+\mu)} \approx \mu x^{-(1+\mu)} & x < x_{\max} \\ 0 & x > x_{\max}. \end{cases} \quad (10.14)$$

That is, we merely cut off the single step distribution at a point beyond which a larger step will almost surely not occur within N steps.

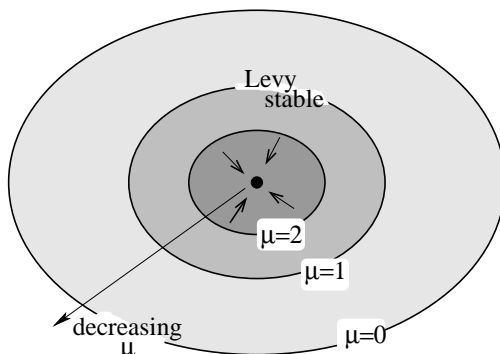


Figure 10.2: Schematic illustration of the universality classes of a random walk when the length x of single step is distributed according to $p(x) \sim x^{-(1+\mu)}$. For $\mu > 2$, all distributions flow to the Gaussian fixed point (heavy dot). For $1 < \mu < 2$, there is normal behavior for the mean displacement and anomalous behavior for the variance. For $\mu < 1$, the first two moments are both anomalous and the Lévy distribution describes the distribution of displacements.

A crucial point about this truncated distribution is that it satisfies the conditions of the central limit theorem—both $\langle x \rangle$ and $\langle x^2 \rangle$ are finite because of the cutoff. We can now exploit this fact to compute the properties of the random walk after N steps. For the mean and mean-square displacement after a single step, we have

$$\langle x \rangle_N \approx \mu \int_1^{x_{\max}} x x^{-(1+\mu)} dx \propto \begin{cases} x_{\max}^{1-\mu} \propto N^{(1-\mu)/\mu} & \mu < 1; \\ \ln x_{\max} \propto \ln N & \mu = 1; \\ \text{finite} & \mu > 1. \end{cases} \quad (10.15)$$

$$\langle x^2 \rangle_N = \mu \int_1^{x_{\max}} x^2 x^{-(1+\mu)} dx \propto \begin{cases} x_{\max}^{2-\mu} \propto N^{(2-\mu)/\mu} & \mu < 2; \\ \ln x_{\max} \propto \ln N & \mu = 2; \\ \text{finite} & \mu > 2. \end{cases} \quad (10.16)$$

Here we write the subscript N on $\langle x \rangle_N$ to emphasize that this mean value for a single steps depends on the number of steps over which the average is taken. Then the mean displacement and the variance of an N -step random walk are simply

$$\langle X_N \rangle = N \langle x \rangle_N \propto \begin{cases} N^{1/\mu} & \mu < 1; \\ N \ln N & \mu = 1; \\ N & \mu > 1. \end{cases} \quad (10.17)$$

$$\text{var}(X_N) \propto \begin{cases} N^{2/\mu} & \mu < 2; \\ N \ln N & \mu = 2; \\ N & \mu > 2. \end{cases} \quad (10.18)$$

In the regime $\mu > 2$, both $\langle x \rangle$ and $\langle x^2 \rangle$ are finite, and the probability distribution after N steps is universally a Gaussian distribution for any single-step distribution whose upper tail decays more quickly than x^{-2} . In the regime $0 < \mu < 2$, the displacement after N is governed by the *Lévy stable* distribution that is often written as L_μ . The most important feature of this distribution is that it has a power-law tail, $L_\mu(z) \sim z^{-(1+\mu)}$. For $\mu < 1$, the scaling variable $z = X_N/N^{1/\mu}$ obeys the Lévy distribution, while for $1 < \mu < 2$, the scaling variable $z = (X_N - N\langle x \rangle)/N^{2/\mu}$ obeys the Lévy distribution. Notice that for $\mu < 1$, the dependence of $\langle X_N \rangle$ on N is the same as x_{\max} ! Thus a single step in the random walk dominates the behavior of the mean displacement.

Heterogeneous waiting times

Another natural way that a random walk can be heterogeneous is to have the time between successive steps drawn from an arbitrary distribution. If the distribution of times τ between steps (the waiting time distribution) is sufficiently sharp that the mean waiting time is finite, then we may anticipate normal diffusive behavior. However suppose that the waiting time distribution has the form $q(\tau) \sim \tau^{-(1+\mu)}$, with $0 < \mu < 1$. Then $\langle \tau \rangle = \infty$, and we should expect slower than normal diffusive behavior. We can again determine the asymptotic behavior of random walks with a broad waiting time distribution by making a correspondence to a process with a suitably truncated waiting time distribution.

For $0 < \mu < 1$, the maximum waiting time over N steps is given by the extremal condition

$$\int_{\tau_{\max}}^{\infty} \tau^{-(1+\mu)} d\tau = \frac{1}{N},$$

from which the maximum waiting time is $\tau_{\max} \propto N^{1/\mu}$. With this truncated waiting time distribution, the average time for a random walk to take one step is then

$$\langle t \rangle_N = \int_0^{\tau_{\max}} \tau \tau^{-(1+\mu)} d\tau \propto \tau_{\max}^{1-\mu} \propto \begin{cases} N^{(1-\mu)\mu} & \mu < 1; \\ \ln N & \mu = 1. \end{cases}$$

Again, the subscript N denotes that this average time pertains only for the first N steps of the walk. Now the total time T_N required to take N steps is given by

$$T_N = N \langle t \rangle_N \propto \begin{cases} N^{1/\mu} & \mu < 1; \\ N \ln N & \mu = 1. \end{cases} \quad (10.19)$$

Finally, the mean-square displacement after N steps of a random walk with a waiting time distribution is

$$\langle X_N^2 \rangle \propto N \propto \begin{cases} T_N^\mu & \mu < 1 \\ T_N / \ln T_N & \mu = 1 \\ T_N & \mu > 1. \end{cases} \quad (10.20)$$

The first case corresponds to *subdiffusion*, where the mean-square displacement grows more slowly than linearly with time.

10.3 Random Walk in a Random Potential

There are two types of disorder that can arise in a random walk problem. The first is the randomness of the individual steps in the walk. The physical mechanism for this randomness is generally the result of thermal noise; the random walker is buffeted by the collisions with other particles in the system and these collisions are normally modeled by assuming the each step of the walker is in a random direction. As we already discussed briefly in chapter 2, there are well-developed techniques to deal with this type of randomness and solve for the probability distribution of a random walk.

On the other hand, environmental disorder arises in many contexts. That is, the medium in which the random walker is moving has transport characteristics that do not vary in time but are a random function of position. Such quenched disorder profoundly affects the motion of a random walk. In this section, we discuss one important such example in which the particle can be viewed as moving in a random potential.

The physical mechanism that leads to such a potential arises in the dynamics of a one-dimensional spin glass in which the interactions can take only the values distribution $\pm J$. Suppose that the system is in a uniform weak magnetic field H and that the temperature is low. Because the domain wall density is small in the low-temperature limit, let us focus on the dynamics of a single domain wall. In the case of a spin glass, the notion of a domain wall has to be generalized to account for both ferromagnetic and antiferromagnetic interactions. For a ferromagnetic interaction, the presence of the domain wall that occupies the bond between two spins implies that these spins are antiparallel. Conversely, for an antiferromagnetic interaction, a domain wall implies that the spins at the end of the bond are parallel. The result is that a single domain wall on the k^{th} bond undergoes a random walk in which the hopping rates to the right (p_k) and left ($q_k = 1 - p_k$) are *random* (Fig. 10.3. In the case of low-temperature Glauber kinetics, $p_k = \frac{1}{2}(1 + \epsilon\sigma_k)$, $q_k = \frac{1}{2}(1 - \epsilon\sigma_k)$, where $\sigma_k = \pm$ are independent identically distributed random variables and $\epsilon = \tanh(H/T)$, with H the magnetic field at T the temperature. The temperature must be low, $T \ll J$, to ensure that the creation of new domain walls is exponentially unlikely; the requirement $\epsilon \lesssim 1$ shows that the magnetic field should be of the order of the temperature: $H \sim T$.

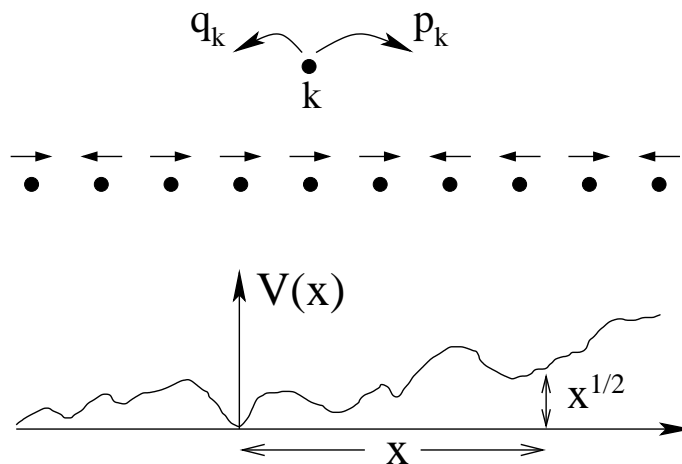


Figure 10.3: (top) The local hopping bias at site k , with p_k and q_k , the probabilities of hopping to the right and left. (middle) The local bias on a string of sites. (bottom) The random potential that is induced by the local bias.

In the continuum limit, the motion of this random walker that is subject to this random bias in space and to random noise can be described by the Langevin equation

$$\frac{dx}{dt} = -f[x(t)] + \eta(t)$$

where $\eta(t)$ is the (Gaussian white) noise and $f(x)$ is the random bias with mean zero and the correlation length of the order of the lattice constant. In one dimension, we can always write the bias as the gradient of a potential $f(x) = -\frac{dV(x)}{dx}$. By definition, the random potential is the integral of the random bias. Since the bias itself has zero mean and rapidly decaying correlations, the random potential has diffusive height fluctuations

$$V(x) - V(0) \sim x^{1/2}.$$

The particle thus moves in a random potential; to move a distance L from its original location, the particle must overcome a potential barrier whose height is of the order of $L^{1/2}$. The probability for this event is just given by the Boltzmann factor and the time needed for such an event to occur is therefore

$$t \propto e^{L^{1/2}}.$$

Thus we conclude that the typical length scale of the random walk grows as

$$L \sim (\ln t)^2. \quad (10.21)$$

It is important to appreciate that an arbitrarily small random bias makes a huge difference in the motion of a random walk—instead of the diffusive growth $L \sim \sqrt{t}$ the particle follows the ultraslow Sinai logarithmic law $L \sim (\ln t)^2$.

Another remarkable manifestation of the influence of a random potential on random walk motion arises when two non-interacting random walkers are subject to the same random potential. If there was no disorder, the positions of the two walkers would be given by

$$\langle x_1^2 \rangle = \langle x_2^2 \rangle = t, \quad \langle (x_1 - x_2)^2 \rangle = 2t;$$

that is, the distance between the two particles also diffuses, but with twice the diffusion coefficient of the single-particle motion. The disorder completely changes the situation—now the interparticle distance reaches a stationary distribution! The origin of this unexpected behavior is that each particle tends to move to near the bottom of its local valley. As time increases, a particle moves to the bottom of progressively deeper valleys. At some point, both particles move to the same valley and then their subsequent positions are strongly correlated because both particles tend to be in the same local valley.

To justify the above picture and derive quantitative results it is useful to take a piecewise linear potential.¹ We can further assume that the slopes are alternatively positive and negative. Let l_n is the length of the n^{th} bond along which the potential grows linearly from V_n to V_{n+1} , so the end points are separated by the barrier $B_n = |V_n - V_{n+1}|$. When the particle moves in such a potential, it will typically sit near the bottom of a valley. If the barrier is small, the particle will soon overcome it and get into a deeper valley. The key point is that on the long time scale, the particle essentially does not see low barriers. This suggests the following recursive procedure that simplifies the random potential yet does not affect the asymptotic characteristics of the particle. At each step, we eliminate the bond (l, B_{\min}) with the smallest barrier by merging it with the adjacent bonds (l_1, B_1) and (l_2, B_2) . This procedure (often called the **decimation method**, or a variant of a **real space renormalization group** method) is illustrated on the figure; it is formally defined via the rule

$$(l_1, B_1) \oplus (l, B_{\min}) \oplus (l_2, B_2) \longrightarrow (l_1 + l + l_2, B_1 - B_{\min} + B_2) \quad (10.22)$$

The procedure preserves the zigzag structure. The crucial feature that makes analysis possible is that correlations do not spontaneously develop: If the barriers were initially uncorrelated, they remain uncorrelated. Overall, (10.22) is an example of the extremal dynamics.

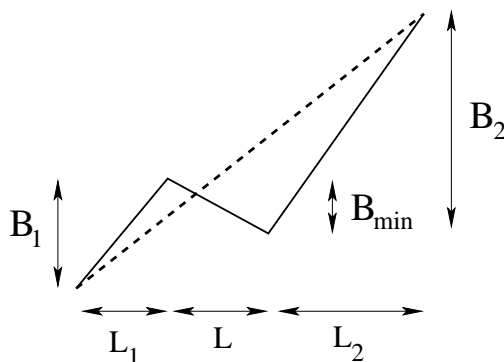


Figure 10.4: The decimation method — the bond with the smallest barrier B_{\min} is eliminated via merging with the adjacent bonds.

Let's first disregard the length and focus on the barrier distribution $c(B, b)$ defined as the number density of bonds with barrier B when the minimal barrier is equal to b . The total bond density $\rho(b) = \int_b^\infty dB c(B, b)$

¹This assumption does not affect the asymptotic behavior.

satisfies

$$\frac{d\rho(b)}{db} = -2c(b, b) \quad (10.23)$$

since three bonds are lost and one is gained in each merging event. Similarly the governing equation for the barrier distribution is

$$\frac{\partial}{\partial b} c(B, b) = c(b, b) \left[-2 \frac{c(B, b)}{\rho(b)} + \int_b^B dB' \frac{c(B', b)}{\rho(b)} \frac{c(B - B' + b, b)}{\rho(b)} \right]$$

In these equations, the minimal barrier height should be thought as the time-like variable. The minimal height is more convenient than time in intermediate calculations. Using the Arrhenius estimate $t \propto e^b$ we can express b through time²

$$b \rightarrow \ln t \quad (10.24)$$

and thereby re-express final results in terms of the original time variable.

When $b \rightarrow \infty$, the barrier distribution approaches the scaling form

$$\frac{c(B, b)}{\rho(b)} \rightarrow b^{-1} \Phi(z), \quad z = \frac{B - b}{b} \quad (10.25)$$

This scaling ansatz recasts the governing equation for the barrier distribution into

$$(1 + z) \frac{d\Phi(z)}{dz} + \Phi(z) + \Phi(0) \int_0^z dx \Phi(x) \Phi(z - x) = 0 \quad (10.26)$$

We could solve this equation by utilizing the Laplace transform that would transform the convolution into the product. Even simpler is to notice that Eq. (10.26) is identical to the equation for the scaling function that appeared earlier when we studied the constant-kernel aggregation. Either way, we arrive at the exponential distribution

$$\Phi(z) = e^{-z} \quad (10.27)$$

Now using $\frac{c(b, b)}{\rho(b)} = b^{-1}$ in conjunction with (10.23), we determine the total bond density $\rho(b) = b^{-2}$ and the density of the bonds with the smallest barrier $c(b, b) = b^{-3}$.

To probe the length distribution we cannot merely study $c(l, b)$ since the dynamics is driven by eliminating the bond of the smallest barrier. Therefore we have to examine $c(l, B, b)$, the number density of bonds of length l and of barrier height B . This joint distribution evolves according to equation

$$\left(\frac{\partial}{\partial b} + 2 \frac{c(b, b)}{\rho(b)} \right) c(l, B, b) = \int dl_1 dl_2 dl_3 \delta(l_1 + l_2 + l_3 - l) \int dB_1 dB_2 \delta(B_1 + B_2 - b - B) \Pi$$

with the integrand $\Pi = c(l_3, b, b) \frac{c(l_1, B_1, b)}{\rho(b)} \frac{c(l_2, B_2, b)}{\rho(b)}$ and the delta functions assuring that the rule (10.22) is obeyed. When $b \rightarrow \infty$, the joint distribution admits the scaling form

$$c(l, B, b) \rightarrow b^{-5} \Phi(w, z), \quad w = b^{-2} l \quad \text{and} \quad z = b^{-1} (B - b)$$

which is understood by noting that the minimal barrier height b sets the scale for B and the inverse bond density $\rho^{-1} = b^2$ sets the scale for l . By inserting the scaling form into the governing equation for $c(l, B, b)$ we find that the scaling function satisfies

$$3\Phi + (1 + z) \frac{\partial \Phi}{\partial z} + 2w \frac{\partial \Phi}{\partial w} + \int dw_1 dw_2 dw_3 \delta(w_1 + w_2 + w_3 - 1) \int dz_1 dz_2 \delta(z_1 + z_2 - z) \Pi = 0$$

with $\Pi = \Phi(w_1, z_1) \Phi(w_2, z_2) \Phi(w_3, 0)$. The Laplace transform $\Phi(p, z) = \int_0^\infty dw e^{-pw} \Phi(w, z)$ converts the above equation into

$$\left[1 + (1 + z) \frac{\partial}{\partial z} - 2p \frac{\partial}{\partial p} \right] \Phi(p, z) + \Phi(p, 0) \int_0^z dx \Phi(p, x) \Phi(p, z - x) = 0 \quad (10.28)$$

²Note that Eq. (10.24) is asymptotically *exact*.

This equation is a generalization of (10.26) whose solution is exponential, Eq. (10.27). This suggests to seek again an exponential solution

$$\Phi(p, z) = \alpha(p) e^{-z\beta(p)} \quad (10.29)$$

Plugging (10.29) into (10.28) we find that the exponential ansatz is compatible with (10.28) when

$$2p \frac{d\alpha}{dp} - \alpha = -\alpha\beta, \quad 2p \frac{d\beta}{dp} - \beta = -\alpha^2 \quad (10.30)$$

By definition, $\Phi(p=0, z) = \int_0^\infty dw \Phi(w, z) = \Phi(z) = e^{-z}$, see (10.27). Therefore $\alpha(0) = \beta(0) = 1$. We can get rid of the linear terms in (10.30) and make the coefficients independent of p . Indeed, the transformation

$$\alpha(p) = qA(q), \quad \beta(p) = qB(q), \quad q = \sqrt{p}$$

converts (10.30) into

$$\frac{dA}{dq} = -AB, \quad \frac{dB}{dq} = -A^2$$

These equations admit the integral $B^2 - A^2 = \text{const.}$, and the solutions are qualitatively different depending on whether the constant positive, zero, or negative. Only the former case leads to physically acceptable solutions. For instance, if the constant were zero we would have obtained $A = B = \frac{A(0)}{1+qA(0)}$ and therefore $\alpha = \beta = \frac{A(0)\sqrt{p}}{1+A(0)\sqrt{p}}$ which disagrees with the boundary condition $\alpha(0) = \beta(0) = 1$. The relevant solution is $A = (\sinh q)^{-1}$ and $B = \coth q$; in the original variables

$$\alpha(p) = \frac{\sqrt{p}}{\sinh \sqrt{p}}, \quad \beta(p) = \sqrt{p} \frac{\cosh \sqrt{p}}{\sinh \sqrt{p}} \quad (10.31)$$

Thus $\Phi(p, z)$ is given by (10.29), (10.31); the inverse Laplace transform of $\Phi(p, z)$ gives $\Phi(w, z)$. The result is cumbersome, so let's limit ourselves to single-variable distributions. We already know $\Phi(z)$, so we want to determine $\Psi(w)$, the scaling form of the length distribution. Of course, $\Psi(w) = \int dz \Phi(w, z)$; the same holds for the Laplace transforms $\Psi(p) = \int dz \Phi(p, z)$. From (10.29) we find $\Psi(p) = \alpha(p)/\beta(p) = [\cosh \sqrt{p}]^{-1}$. The inverse Laplace transform is determined by utilizing the standard tools from complex analysis, that is by finding the poles of $\Psi(p)$ and calculating the residues. The scaled length distribution reads

$$\begin{aligned} \Psi(w) &= \pi \sum_{n=-\infty}^{\infty} (-1)^n \left(n + \frac{1}{2}\right) \exp \left\{ -\pi^2 w \left(n + \frac{1}{2}\right)^2 \right\} \\ &= \frac{1}{\pi^{1/2} w^{3/2}} \sum_{n=-\infty}^{\infty} (-1)^n \left(n + \frac{1}{2}\right) \exp \left\{ -\frac{1}{w} \left(n + \frac{1}{2}\right)^2 \right\} \end{aligned} \quad (10.32)$$

Here we gave the answer in two equivalent forms which are convenient in extracting large and small w behaviors, respectively.

The qualitative features of the random walks in the random environments outlined at the beginning of this section can now be expressed in a quantitative form. Let $\text{Prob}(x, t|0, 0)$ is the probability that a particle starting at the origin is located at x at time t . We argued that in a single environment the particle will be at the bottom of the renormalized bond that contains the origin. We want to compute the average over the environments: $\overline{\text{Prob}(x, t|0, 0)}$. If $P(l, b)$ is the probability that the length of the renormalized bond is l , then the particle will be in such bond with probability $l P(l, b) / \int dl \ell P(\ell, b)$. The bottom of the valley is uniformly distributed on $[0, l]$, so bonds of length $l \geq |x|$ contribute to $\overline{\text{Prob}(x, t|0, 0)}$:

$$\overline{\text{Prob}(x, t|0, 0)} = \left[2 \int_0^\infty dl \ell P(\ell, b) \right]^{-1} \int_{|x|}^\infty dl P(l, b)$$

We know that $P(l, b) \rightarrow b^{-2} \Psi(l/b^2)$ with $\Psi(w)$ given by (10.32). Using this and recalling that $b = \ln t$, see Eq. (10.24), we arrive at

$$\overline{\text{Prob}(x, t|0, 0)} = (\ln t)^{-2} F(X), \quad X = \frac{x}{(\ln t)^2}$$

with

$$F(X) = \frac{2}{\pi} \sum_{n=0}^{\infty} (-1)^n \left(n + \frac{1}{2}\right)^{-1} \exp \left\{ -\pi^2 |X| \left(n + \frac{1}{2}\right)^2 \right\}$$

This Golosov-Kesten distribution replaces the Gaussian distribution characterizing the displacement of the ordinary random walk. Although the Golosov-Kesten distribution is an infinite series, the moments of the displacement (averaged over the noise and the environments) are remarkably simple, e.g.,

$$\overline{\langle x^2 \rangle} = \frac{61}{180} (\ln t)^4, \quad \overline{\langle x^4 \rangle} = \frac{50521}{75600} (\ln t)^8, \quad \overline{\langle x^6 \rangle} = \frac{199360981}{60540480} (\ln t)^{12}$$

We already mentioned the remarkable phenomenon of localization — two particles remain within the finite distance even when $t \rightarrow \infty$, that is the probability distribution $P(y, t)$ of the interparticle distance $y(t) = x_1(t) - x_2(t)$ averaged over the environments reaches a stationary limit distribution $P_{\infty}(y)$. The existence of the limit distribution does not imply, however, that all moments of y are finite. An algebraic tail of the limit distribution

$$P_{\infty}(y) \sim |y|^{-3/2} \quad \text{as} \quad |y| \rightarrow \infty \quad (10.33)$$

leads to formal divergence of the moments. At any finite time, of course, the distribution $P(y, t)$ vanishes for $|y| \gg (\ln t)^2$. Hence the second moment of the interparticle distance³ grows as

$$\overline{\langle y^2 \rangle} \sim \int^{(\ln t)^2} dy y^{-3/2} y^2 \sim (\ln t)^3$$

and more generally $\overline{\langle y^n \rangle} \sim (\ln t)^{2n-1}$ for even n . To understand the algebraic tail (10.33) we recall that the particles are at the deepest valleys of the renormalized bond that contains the starting point. There could be two valleys of (almost) same depth separated by distance y . The probability of this event is estimated by noting that the random potential $U(y)$ undergoes a random walk, and the probability that this random walk returns to the origin (i.e., $U(y)$ gets close to $U(0)$) is the first-passage probability that indeed scales as $y^{-3/2}$ for large y .

10.4 Random Walk in Random Velocity Fields

The motion of a random walk in a random medium often can be **subdiffusive**, that is the mean-square displacement $\langle \mathbf{r}^2(t) \rangle$ grows slower than linearly with time. Spatial disorder in the hopping rates of the random walk is a natural mechanism that gives rise to subdiffusion. Conversely, there are situations where **superdiffusive** motion can occur, in which $\langle \mathbf{r}^2(t) \rangle$ grows faster than linearly with time. A simple such example is the Matheron-de-Marsily (MdM) model that was formulated to describe groundwater transport in sedimentary rocks.

In the MdM model, a sedimentary rock is modeled as an array of parallel layers, each with slightly different material properties (Fig. 10.5). In each sedimentary layer, the fluid moves at a velocity that is characteristic of that layer. In a reference frame that moves at the average velocity of all the layers, the relative velocity in each layer becomes a random, zero-mean function of the transverse position. Now consider the motion of a Brownian particle that is also passively convected by the flow field. When the particle remains within a given layer, it moves at the fluid velocity in the layer, but the particle also undergoes superimposed molecular diffusion. Because of diffusion the particle will make transitions between neighboring layers and so its longitudinal velocity will change in a stochastic manner. This combination of transverse diffusion and random flow in the longitudinal direction leads to superdiffusion.

In two dimensions, with convection along the x -axis and diffusion along the y -axis, the equations of motion for a Brownian particle are

$$\frac{dx}{dt} = u[y(t)], \quad \frac{dy}{dt} = \eta(t), \quad (10.34)$$

with $u[y(t)]$ the velocity field in the x -direction that depends only on transverse position y . To simplify the system even further, we replace the continuum picture of Fig. 10.5(b) by the discrete picture of Fig. 10.5(c)

³We can, of course, express $\overline{\langle y^2 \rangle}$ via the one-particle averages $\overline{\langle y^2 \rangle} = 2 \overline{\langle x^2(t) \rangle} - \overline{\langle x(t) \rangle^2}$

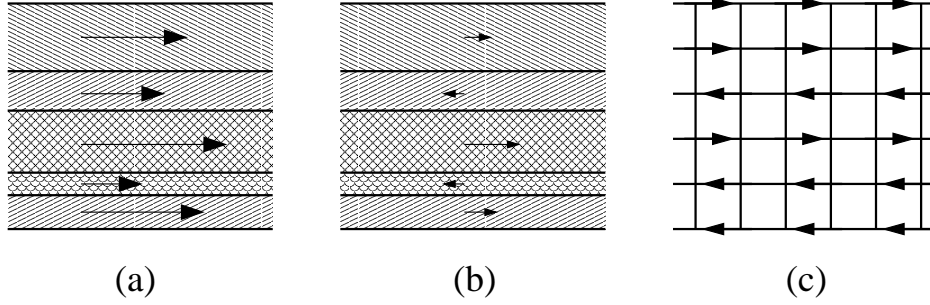


Figure 10.5: (a) The flow field in a two-dimensional layered medium and (b) the same flow in a center-of-mass reference frame, from which we abstract the MDM model shown in (c).

in which the velocity in each layer is randomly $\pm u_0$. By construction the mean velocity equals zero and there are no correlations between the velocities in different layers, so that

$$\langle u(y) \rangle = 0, \quad \langle u(y)u(y') \rangle = \sigma\delta(y - y').$$

The effect of diffusion in the x -direction is subdominant with respect to the random convection and therefore may be ignored. The transverse diffusion of the particle is driven by thermal noise that satisfies

$$\langle \eta(t) \rangle = 0, \quad \text{and} \quad \langle \eta(t)\eta(t') \rangle = 2D\delta(t - t').$$

We can determine the time dependence of the longitudinal mean-square displacement by the following simple argument. Let us first estimate the effective longitudinal bias that the Brownian particle has experienced up to time t . If every layer in the system was visited with equal frequency, then the mean bias would be zero. However, a diffusing particle can visit only a finite number of layers within which the mean bias can be non-zero. This residual bias is responsible for superdiffusion. In a time t , a particle typically roams over a perpendicular distance \sqrt{Dt} . Since $u(y)$ is a random function with zero mean, the residual bias within this spatial range \sqrt{Dt} is

$$\langle u \rangle_t = \frac{1}{\sqrt{Dt}} \sum_{\sqrt{Dt}} u(y) \sim u_0(Dt)^{-1/4}. \quad (10.35)$$

Thus we estimate that the root-mean-square longitudinal displacement at time t , $x_{\text{rms}}(t) = \langle x^2(t) \rangle^{1/2}$, grows superdiffusively

$$x_{\text{rms}}(t) \sim \langle u \rangle_t t \sim u_0 D^{-1/4} t^{3/4}. \quad (10.36)$$

A more fundamental characteristic of the particle motion is the probability distribution of displacements. When averaged over all particle trajectories and over all realizations of the velocity disorder, we expect that this displacement distribution at long times should have the scaling form

$$P(x, t) \rightarrow t^{-3/4} f(xt^{-3/4}). \quad (10.37)$$

In terms of the natural variable is $\xi \equiv xt^{-3/4}$, the natural expectation for the scaling function is that it should decay faster than any power law for $\xi \gg 1$. Thus we write

$$f(\xi) \sim t^{-3/4} e^{-a\xi^\delta}, \quad (10.38)$$

with a a constant. There is a very simple, general, and powerful argument to determine the shape exponent δ . Let us first outline this method for standard diffusion and then extend this approach to the MDM model. Suppose that we know that $\langle r(t)^2 \rangle$ scales linearly with time, but that we don't know that the probability distribution is Gaussian; we only know that the distribution satisfies scaling. To make the argument more general we write $\langle r(t)^2 \rangle \sim t^{2\nu}$ to also encompass situations where the distance exponent ν does not equal $1/2$. With the assumption of scaling, we expect that the probability distribution of displacements will be

$$P(r, t) \rightarrow t^{-d\nu} e^{-a(r/t^\nu)^\delta}. \quad (10.39)$$

A very useful general trick to determine the shape exponent δ is to consider the subset of extreme, stretched-out walks for which $r \sim t$. For a walk to be stretched out, each step must be in the same direction. The probability for this event to occur decays exponentially with the number of steps, since the walk must pick only one out of the available choices of direction at each step. Thus we have

$$P(r \sim t, t) \rightarrow t^{-d\nu} e^{-a(t^{1-\nu})^\delta} \sim e^{-t}.$$

By comparison, we thus infer the fundamental relation between the shape exponent and the distance exponent

$$\delta = \frac{1}{1-\nu}. \quad (10.40)$$

Thus for diffusion, where $\nu = 1/2$, we obtain the expected Gaussian value of $\delta = 2$. Moreover, this argument applies for a wide variety of situations. A crucial feature of this trick is to consider an extremal subset of all trajectories for which it is trivial to estimate their probability. It is then a simple matter to compare the probability of this extremal subset with the probability that arises from the scaling form to determine the shape exponent.

Let's now try the same approach for the MdM model. Here it is simplest to formulate the extremal argument for a discretized lattice version of the MdM model in which the velocity for a given value of y is independently equal to ± 1 . In this case, there is a subtlety in applying the extremal argument because there are two sources of disorder—the disorder in the trajectory and the disorder in the medium. What are the configurations that lead to an extremal walk? Clearly, the walk travels furthest longitudinally if it is contained within a range of y values that all have the same velocity of $+1$. What is the probability for such an event? This confining probability, averaged over all environments, is isomorphic to the survival probability of a one-dimensional random walk in the presence of randomly distributed traps that was discussed in Sec. 8.5. If the unidirectional region has a width w , the probability for such a region is simply 2^{-w} . In the long-time limit, the probability for a walk to remain within this region decay as e^{-Dt/w^2} . The confining probability, averaged over all widths, is then $\int 2^{-w} e^{-Dt/w^2} dw$, which varies as $e^{-at^{1/3}}$. Now using the scaling form (10.38) for the probability distribution in the MdM model and applying the same comparison as in Eq. (10.4), we have

$$P(x \sim t, t) \rightarrow t^{-3/4} e^{-at^{\delta/4}} \sim e^{-t^{1/3}},$$

from which we infer that the shape exponent δ has the value $\delta = 4/3$. A surprising feature of the MdM model is that the shape and distance exponents do not obey the general relation $\delta = \frac{1}{1-\nu}$.

In addition to the superdiffusive transport exhibited by this layered model, there is a lack of self averaging. That is, the asymptotic rate at which the probability distribution spreads in a single environment is different from the spread rate when an average over all environments is taken. This feature can be seen in computing the higher moments of the longitudinal displacement. The moment of arbitrary order can be written formally as,

$$\langle\langle x^n(t) \rangle\rangle_w = n! \int_0^t dt_1 \int_0^{t_1} dt_2 \cdots \int_0^{t_{n-1}} dt_n \langle\langle u(y(t_1)) \cdots u(y(t_n)) \rangle\rangle_w. \quad (10.41)$$

The double angle brackets indicate that one should first average over all transverse Brownian trajectories for a given configuration of random velocities, and then average over all configurations. However, these two averages factorize and can be performed in either order. Thus the velocity correlation function can be written as

$$\begin{aligned} \langle\langle u(y(t_1)) \cdots u(y(t_n)) \rangle\rangle_w &= \int_{-\infty}^{+\infty} dy_1 dy_2 \cdots dy_n \langle u(y_1) \cdots u(y_n) \rangle_c \\ &\times p(y_n, t_n) p(y_{n-1} - y_n, t_{n-1} - t_n) \cdots p(y_1 - y_2, t_1 - t_2), \end{aligned} \quad (10.42)$$

where $p(x, t) = \frac{1}{\sqrt{4\pi Dt}} e^{-x^2/4Dt}$ is the Gaussian probability distribution for the transverse motion. The product of Gaussians in Eq. (10.42) is the probability that a Brownian path visits the sequence of transverse positions $\{y(t_i)\}$ at times $\{t_i\}$, having started at $y = 0$. For the continuous model defined by Eq. (10.34), $\langle u(y_1) \cdots u(y_n) \rangle_c$ is a sum of products of delta functions. Consequently, the second moment is

$$\langle\langle x(t)^2 \rangle\rangle_w = 2\sigma \int_0^t dt_1 \int_0^{t_1} dt_2 \int_{-\infty}^{+\infty} dy p(0, t_1 - t_2) p(y, t_2) = \frac{4\sigma}{3\sqrt{\pi D}} t^{3/2}. \quad (10.43)$$

On the other hand, the longitudinal displacement, averaged over all walks in a *fixed* environment, $\langle x(t) \rangle_w$, depends on the configuration, and does not necessarily converge to zero at large times. However, the average over all environments, $\langle \langle x(t) \rangle_w \rangle_c$ does equal zero in the center-of-mass reference frame. Clearly $\langle x(t) \rangle_w$ has a distribution over environments which is a Gaussian of variance $\langle \langle x(t) \rangle_w^2 \rangle_c$. This dispersion can also be calculated for the continuous model of Eq. (10.34),

$$\langle \langle x(t) \rangle_w^2 \rangle_c = \sigma \int dy \langle \mathcal{N}(y, t) \rangle_w^2 = (\sqrt{2} - 1) \frac{4\sigma}{3\sqrt{\pi D}} t^{3/2}, \quad (10.44)$$

where $\mathcal{N}(y, t) = \int_0^t dt' \delta(y - y(t'))$ is the number of times that the random walk $y(t)$ visits layer y after time t , having started at $y = 0$. Thus both the configuration average of the mean-square displacement, $\langle \langle x(t) \rangle_w^2 \rangle_c$ and the second moment $\langle \langle x(t) \rangle_w^2 \rangle_c$ vary as $t^{3/2}$, but *with different prefactors*. This implies that there are non-vanishing sample specific fluctuations in the variance, asymptotically, and hence in the probability distribution itself.

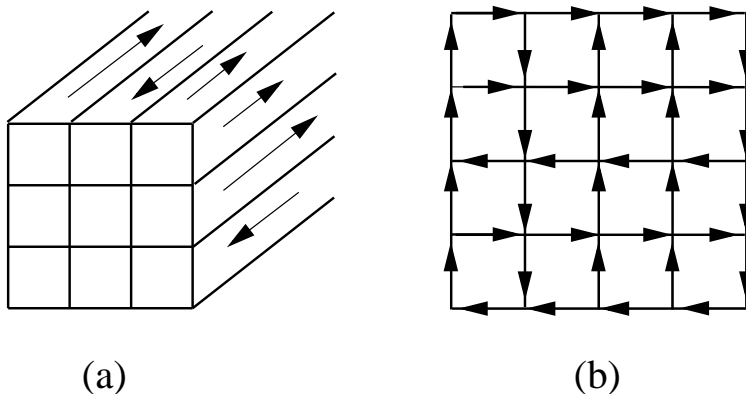


Figure 10.6: (a) The flow field of the MDM model in three dimensions. (b) The isotropic version of the MDM model—the random Manhattan grid—in two dimensions.

What happens in the MDM model for the physical case of three dimensions? There are two situations that could be considered: parallel sedimentary slabs or sedimentary filaments (Fig. 10.6). The former case is perhaps more physical but it has the same behavior as the two-dimensional system. The latter case is what we term the three dimensional MDM model. Now the equations of motion for a Brownian particle are

$$\frac{dx}{dt} = u[y_1(t), y_2(t)], \quad \frac{dy_1}{dt} = \eta_1(t), \quad \frac{dy_2}{dt} = \eta_2(t).$$

Once again, it is helpful to think of a lattice model in which there are random velocities in the x -direction that take on the values $\pm u_0$ equiprobably and that the velocity has the same value for a fixed value of the transverse coordinates y_1 and y_2 . To determine the longitudinal displacement, it is again helpful to decompose the longitudinal and transverse motions. In the transverse direction, the trajectory of the particle is that of a pure random walk in two dimensions. From classic results about random walks in two dimensions, we know that the particle typically visits of the order of $t/\ln t$ distinct sites in the transverse subspace. Thus the mean bias that the walk experiences is given by the extension of Eq. (10.35) to three dimensions:

$$\langle u \rangle_t = \frac{1}{t/\ln t} \sum^{t/\ln t} u(y) \sim \sqrt{\frac{\ln t}{t}}. \quad (10.45)$$

Then we simply estimate the rms displacement to be

$$x_{\text{rms}}(t) \sim \langle u \rangle_t t \sim (t \ln t)^{1/2}.$$

As a final note, the MDM model can be generalized to an isotropic random velocity field in which superdiffusion again occurs. An amusing example is the “random Manhattan” square lattice, in which the

directionality along any Avenue or Street is fixed along its entire length, but whose orientation is random. The mean-square displacement for a random Manhattan walk can be obtained by a direct generalization of the arguments that led to Eqs. (10.36). We first decompose the isotropic motion into transverse and longitudinal components, and then determine the residual longitudinal bias in a typical region swept out by the transverse Brownian motion. Assuming that $x_{\text{rms}} \sim y_{\text{rms}} \sim t^\nu$, then from Eq. (10.35), the mean longitudinal velocity in the x -direction at time t , averaged over the t^ν layers that a typical random walk visits during its excursions in the y -direction, vanishes as $t^{-\nu/2}$. The from the direct analog of Eq. (10.36), we then conclude that $x_{\text{rms}} \sim t^{1-\nu/2}$. By isotropy, however, one must have $\nu = 1 - \nu/2$, or $\nu = 2/3$. Generalizing this argument to arbitrary spatial dimension d , yields $\nu = 2/(d + 1)$ for $d < d_c = 3$, $\nu = 1/2$ for $d > d_c$, and with logarithmic corrections appearing for $d = d_c$.